Atmos. Chem. Phys. Discuss., https://doi.org/10.5194/acp-2018-778
Manuscript under review for journal Atmos. Chem. Phys.
Discussion started: 28 August 2018

Atmospheric Chemistry and Physics
Discussions

Evolutionary Characteristics of Lightning and Radar Echo Structure in Thunderstorms Based on the TRMM satellite

Xueke Wu[1], Tie Yuan[1], Rubin Jiang[2], Jinliang Li[1]

[1]College of Atmospheric Sciences and Key Laboratory for Semi-Arid Climate Change of the Ministry of Education, Lanzhou University, Lanzhou 730000, China

[2]Key Laboratory of Middle Atmosphere and Global Environment Observation (LAGEO), Institute of Atmospheric Physics, Chinese Academy of Sciences, Beijing 100029, China

Correspondence:

Dr. Xueke Wu

College of Atmospheric Sciences, Lanzhou University

No. 222, Tianshui Southern Road, Lanzhou 730000 (P.R. China)

Email: wuxk@lzu.edu.cn

Abstract: Based on the 16-years Tropical Rainfall Measuring Mission (TRMM) satellite observational data, the convective characteristics of thunderstorms over different topographic regions, as well as their radar echo structural and lightning activity, are analyzed. The results reveal that thunderstorms over the Tibetan Plateau have weak lightning frequency and small horizontal scale, but their occurrence frequency is the largest, accounting for ~20% of total precipitation events, followed by 10% over the adjacent foothills to the east and hilly land in southern China, with the lowest occurrence frequency (~3%) over the ocean. The 30 dBZ echo top height is a good indicator to predict the occurrence probability of lightning in convective storm, which is more concise and intuitive than the 20 and 40 dBZ echo top heights. Integrating the ratio of convective rainfall to total rainfall and the three-dimensional radar echo structure features to identify thunderstorm life-cycle stages has been proved to be a useful method, and which can help us further explore and maximize the usage of the valuable convective event data from non-geostationary satellites. It is found that the development of dynamic process, which refers to radar echo vertical structure, precedes the lightning activity during the evolution of thunderstorms. Although both lightning activity and radar echo structure peaked at the mature stage, thunderstorms before reaching the mature stage are stronger in radar echo vertical structure while weaker in lightning activity, and vice versa after the mature stage. Even during the dissipating stage of thunderstorm, there still some lightning was observed.

Atmos. Chem. Phys. Discuss., https://doi.org/10.5194/acp-2018-778
Manuscript under review for journal Atmos. Chem. Phys.
Discussion started: 28 August 2018

Atmospheric Chemistry and Physics
Open Access
Discussions

Introduction

Thunderstorms are responsible for the development and formation of many severe weather phenomena, e.g., damaging wind gusts, large hail, flash floods, lightning, and tornadoes, and usually result in serious loss of human property and lives. Moreover, thunderstorms play a vital role in near-surface water and pollutants entering the stratosphere due to vertical convective transport (Park et al., 2007; Randel et al., 2010; Qie et al., 2014). This is a hot scientific topic in recent years with global climate change. However, as thunderstorms usually occur randomly in time and space, which limits the effective detection of thunderstorms, understanding of the thunderstorm formation mechanism and forecasting of thunderstorms still requires more in-depth study.

The Tropical Rainfall Measuring Mission (TRMM) satellite (Kummerow et al., 1998, 2000) was launched in 1997 and officially ended on 15 April 2015 after the spacecraft depleted its fuel reserves. It provided groundbreaking three-dimensional (3D) images of rain and storms for 17 years, far beyond the expected 3–5 year lifetime. Using the long-term and high-quality data from the TRMM satellite, global and regional rainfall, convective systems, and thunderstorms have been widely studied, and many useful and valuable scientific results have been obtained (e.g., Nesbitt et al., 2000; Cecil et al., 2005; Zipser et al., 2006; Liu et al., 2007; Houze et al., 2015). The geographical distribution of the most intense storms (Zipser et al., 2006), deep convection (Liu and Zipser, 2005; Liu et al., 2007), and lightning (Cecil et al., 2014; Albrecht et al., 2016) over the global tropics have been investigated in detail. These studies indicate that the deepest convection mainly occurs over the tropics (Liu and Zipser, 2005; Liu et al., 2007), the highest lightning frequency and most intense storms are mainly found over continental regions, and the highest density of thunderstorms is located in the subtropics (Zipser et al., 2006; Cecil et al., 2014; Albrecht et al., 2016). In addition, the regional, seasonal, and diurnal variations of different types of extreme convection over subtropical South America (Rasmussen et al., 2014), the South Asian region (Romatschke et al., 2010; Qie et al., 2014), and the Himalayan region (Houze et al., 2007; Wu et al., 2016) have been studied. It has been found that the most intense convection occurs upstream of and over the lower elevations of mountain barriers (Houze et al., 2007; Wu et al., 2016), while mesoscale convective systems with the most robust stratiform regions occur primarily in the rainiest season and regions (Romatschke et al., 2010). All these results reveal that the distribution of convection has obvious regional differences, which means that the occurrence and development of convective systems are closely related to regional atmospheric conditions and topographical features.

Many studies (Reynolds et al., 1957; Takahashi, 1978; Jayaratne et al., 1983; Saunderset al., 1991; Bürgesser et al., 2006) have suggested that the juxtaposition of updraft and mixed-phase microphysics (0 to −40ºC) provides favorable conditions where non-inductive charging can efficiently occur via collision and separation between graupel/hail and ice crystals in the presence of supercooled liquid water in thunderclouds. Therefore, lightning activity is closely linked to the dynamic and microphysical processes of thunderclouds and it considered to be an excellent

Atmos. Chem. Phys. Discuss., https://doi.org/10.5194/acp-2018-778
Manuscript under review for journal Atmos. Chem. Phys.
Discussion started: 28 August 2018

indicator for studying convective intensity of vigorous thunderstorm (Ingersoll et al., 2000; Deierling and Petersen, 2008; Qie et al., 2015). A rapid increase in lightning frequency means that the cloud updraft has entered its most vigorous phase and the intense updrafts in thunderclouds usually produce large hail, lightning, heavy rain, tornadoes, and so on. In recent years, lightning data has become an important supplement in the study of severe convective event with the continuous improvement of detection technology, as well as the accumulation of high-quality lightning data. The relationships between lightning flash rate and thundercloud radar reflectivity structure characteristics, such as maximum echo top height (Ushio et al., 2001) and maximum radar reflectivity at different altitudes (Cecil et al., 2005; Pessi and Businger, 2009), have been studied. In addition, the relationship between lightning and precipitation (Petersen and Rutledge, 1998; Takayabu, 2006; Iordanidou et al., 2016; Zheng et al., 2016), ice-water content retrieved from radar reflectivity (Petersen et al., 2005; Deierling and Petersen, 2008), and ice scattering signatures (85 GHz and 37 GHz polarization-corrected temperature) (Toracinta et al., 2002) have also been studied. Based on these reported relationships between lightning and convective properties, a variety of lightning data assimilation techniques have been explored and applied in mesoscale forecast models, which have been shown to be effective in improving simulation results (Mansell et al., 2007; Fierro et al., 2013; Qie et al., 2014). It can be seen that there have been many useful results about lightning and the convective properties of thunderstorms based on observational data from the TRMM satellite, but, a further in-depth study of the interaction and evolution of lightning process and dynamic and microphysical processes is still required, which can deepen the understanding of the formation process of thunderstorms and help improve the effectiveness and reliability of lightning data assimilation techniques. It is generally accepted that the stronger the convective intensity of a thunderstorm, the greater the corresponding lightning flash rate. However, the relationship between lightning flash rate and convective intensity in some thunderstorms does not follow this pattern, especially those convective storm events that can only observe about 80 seconds at a time by non-geostationary satellites (i.e., the TRMM and the GPM). For example, some storms have a strong radar echo structure (maximum reflectivity exceeding 40 dBZ) but no lightning is observed by the lightning imaging sensor (LIS), in contrast, some storms have lightning but the maximum radar reflectivity does not exceed 40 dBZ — a similar situation also occurs in the most intense storms. This has caused some confusion and misunderstanding of the relationship between lightning and convective intensity in thunderstorms.

Accordingly, the purpose of the present study is to investigate the occurrence of lightning in convective systems and the variation in the characteristics of lightning and radar echo structure with the evolution of thunderstorms using the 16-yr TRMM data. The data and method adopted in this study are described first. Then, the characteristics of thunderstorms over different terrain conditions, the occurrence of lightning in convective systems, and the pattern of lightning and intense echo core in three types of the most intense thunderstorms are discussed. Furthermore, a schematic is concluded and established to illustrate the patterns of lightning and radar echo

Atmos. Chem. Phys. Discuss., https://doi.org/10.5194/acp-2018-778
Manuscript under review for journal Atmos. Chem. Phys.
Discussion started: 28 August 2018

structure in different evolution stages of thunderstorms. Finally, the main conclusions are summarized.

2 Data and methods

Convective systems mainly distribute in the tropics while the most intense thunderstorms more locate in subtropical regions, their occurrence and distribution are closely related to the atmospheric circulation and terrain conditions (Zipser et al., 2006; Houze et al., 2007; Wu et al., 2016). Based on this, the subtropical region of East Asia is selected as the study area in this paper. Its specific scope and topographic features are shown in Fig. 1. The study area is further divided into four adjacent subregions from west to east according to the different terrain conditions: the Tibetan Plateau, the eastern foothills, the hilly land in southern China, and the ocean (mainly the coastal ocean).

Information on the convective precipitation systems in this study was extracted from the TRMM precipitation radar (PR) and lightning imaging sensor (LIS) observational data from 1998 to 2013; the data in August 2001 are excluded due to the data-quality issues associated with the TRMM satellite orbit boost (Zipser et al., 2006). The TRMM PR provides the 3D vertical structure features and the LIS provides the lightning flash count and view time of thunderstorms (Kummerow et al., 1998, 2000). To statistically analyze the climatology characteristics of thunderstorms over the study region, it is necessary to identify convective systems in the TRMM PR orbital data. The precipitation features (PFs) from the University of Utah TRMM

Atmos. Chem. Phys. Discuss., https://doi.org/10.5194/acp-2018-778
Manuscript under review for journal Atmos. Chem. Phys.
Discussion started: 28 August 2018

database (http://trmm.chpc.utah.edu/) are adopted in this study, defined by Nesbitt et al. (2000) and Liu et al. (2008) as contiguous TRMM PR 2A25 (Iguchi et al., 2000) near surface raining pixels with rainfall rate > 0. After grouping PR pixels, maximum echo top height with different reflectivities, number of PR pixels, lightning flash counts, view time, etc., inside the PFs are calculated from the collocated orbital data. To limit noise, only PFs with at least four contiguous PR pixels (Liu et al., 2012) are used in this study. Some erroneous cases of PFs, e.g., abnormal and discontinuous echo in vertical profiles (Qie et al., 2014), are also excluded. In this study, thunderstorms are defined as PFs with at least one lightning flash observed by the LIS, non-thunderstorms are defined as PFs without any flash observed.

Many useful results (e.g., Zipser et al., 2006; Liu et al. 2007, 2012; Qie et al., 2014; Wu et al., 2016) have been obtained from satellite data. As is well known, thunderstorms, regardless of type, go through three stages: an initial developing stage, a mature stage, and a dissipation stage. Convective precipitation observed by a satellite that operates in a non-sun-synchronous orbit can be in any of these stages. This may have a negative impact on the relationships between lightning frequency and the convective intensity parameters. However, most studies do not take into account the different stages of thunderstorms when analyzing the relationship between lightning activity and convective properties. Recently, Bang and Zipser (2015) analyzed the distribution of the ratio of convective volumetric rainfall to total (convective plus stratiform) volumetric rainfall based on the TRMM 2A25 product. This study followed the logic used in previous studies (e.g., Houze, 1997;

Romatschke and Houze, 2010; Zuluaga and Houze, 2015) that as a convective system evolves, the young, vigorous convective region matures into widespread convection coexisting with a stratiform region, and finally into mostly stratiform precipitation. A ratio value of 1 means that the storm is 100% convective, which is commonly typified as 'young' convection, whereas a value close to 0 means that the dominant radar precipitation feature (RPF) is stratiform precipitation, which is typified as 'mature' convection (Bang and Zipser, 2015). In this study, the ratio of convective volumetric rainfall to total volumetric rainfall and the PR echo structure characteristics is adopted to distinguish the different stages of thunderstorms, which is beneficial for analyzing the relationship between lightning activity and convective intensity of thunderstorms observed by the TRMM satellite.

3 Results

3.1 Thunderstorms and non-thunderstorms

The occurrence and development of convective precipitation is closely related to the terrain condition. Over the four terrain regions (in Fig. 1), the cumulative distribution function (CDF) for lightning flash rate of RPFs, identified from the TRMM orbit data, is shown in Fig.2. The occurrence frequency of thunderstorms over the Tibetan Plateau is the highest, accounting for about 20% of the total PFs, followed by 10% over the foothills and the hilly land. Only ~3% of PFs over the coastal ocean have lightning. This is generally consistent with the results from a previous study (Liu et al., 2012) which found that the ratio of the RPFs with flashes over land is 11% and

Atmos. Chem. Phys. Discuss., https://doi.org/10.5194/acp-2018-778
Manuscript under review for journal Atmos. Chem. Phys.
Discussion started: 28 August 2018

over the coastal region is 2.66%. Thunderstorms over the Tibetan Plateau are the most frequent; however, the purple line in Fig. 2 indicates that the fraction of thunderstorms over the Tibetan Plateau more rapidly decreases with increasing lightning flash rate compared with the other regions. This means that thunderstorms over the Tibetan Plateau are dominated by weak thunderstorms with less lightning, while the occurrence of intense thunderstorms is relatively scarce. For example, the fraction of intense thunderstorms with a lightning flash rate greater than 100 fl min^{-1} is only 2×10^{-5}, far less than in the other regions. In addition, the lightning flash rate values at the three black dashed lines in Fig. 2 further confirm this conclusion. Lightning activity of thunderstorms over the hilly land is the most active among the study subregions, followed by the foothills region. Over the coastal ocean, although the percentage of 3% is less than the continental regions, it is still more significant than that over open oceans (Liu et al., 2012).

The PR echo structure characteristics of non-thunderstorms and thunderstorms over different subregions based on the TRMM PR data are calculated and shown in Table 1. The vertical and horizontal structures reveal that thunderstorms are significantly taller and larger than non-thunderstorms over all the subregions. From the maximum echo top heights of different reflectivities, especially the strong echo of 40 dBZ, it can be seen that thunderstorms over the hilly land are the most intense, followed by the foothills. The horizontal scale of thunderstorms gradually decreases from the ocean west to the Tibetan Plateau. Although the thunderstorms over the Tibetan Plateau are the most frequent, the vertical and horizontal structures together

Atmos. Chem. Phys. Discuss., https://doi.org/10.5194/acp-2018-778
Manuscript under review for journal Atmos. Chem. Phys.
Discussion started: 28 August 2018

with the lightning flash rate shown in Fig. 2 indicate that thunderstorms over the Tibetan Plateau are the smallest and weakest among the four subregions, which is consistent with the conclusions of previous studies (Luo et al., 2011; Qie et al., 2014). The electrification and discharge processes of thunderstorms are closely related to the mixed-phase region of thundercloud. Accordingly, the maximum PR reflectivity between 6 and 11 km altitude (Maxdbz6-11) is used to demonstrate radar echo intensity characteristics in the mixed-phase region and is also listed in Table 1. Note that the Tibetan Plateau is different from the other subregions due to its very high terrain. The results show that the maximum reflectivity in the mixed-phase region of thunderstorms is about 40 dBZ over the different subregions, which is significantly greater than that of non-thunderstorms.

(Figures 2 and Table 1)

3.2 Convective properties of thunderstorms

The TRMM satellite runs in a non-sun-synchronous orbit, which means that the observed data are just one moment in the life cycle of precipitation events. In other words, those observed convective events include convective storms at all different life stages, i.e., cumulus, mature, and dissipation stages. This may lead to confusion in terms of understanding the relationship between lightning and convective intensity in thunderstorms. The updraft and downdraft play an important role in the evolution of thunderstorms from generation to maturation and eventually to dissipation. In the initial stage of thunderstorms, convective clouds are dominated by ascending motion

Atmos. Chem. Phys. Discuss., https://doi.org/10.5194/acp-2018-778
Manuscript under review for journal Atmos. Chem. Phys.
Discussion started: 28 August 2018

Atmospheric Chemistry and Physics Discussions

and produce convective precipitation. With the evolution of the convective storms, the ascending motion weakens, the descending motion gradually strengthens, and finally the precipitation system is mainly stratiform precipitation when it is dominated by descending motion in the dissipation stage. Accordingly, the ratio of convective volumetric rainfall to total volumetric rainfall of thunderstorms as introduced in section 2 is used to distinguish the life stage of thunderstorms observed by the TRMM satellite. The frequency distribution of the ratio of convective rainfall to total rainfall in thunderstorms over the four different subregions is shown in Fig. 3. The ratio over the Tibetan Plateau is significantly different to the other regions, where the percentage of thunderstorms with less convective precipitation is obviously higher than that over the other subregions, and even 7% of thunderstorms do not have convective rainfall at all. This may be due to the misidentification of rain type by the TRMM PR over the plateau (Fu and Liu, 2007), as the TRMM PR algorithm misidentifies weak convective rainfall events as stratiform rainfall events. Therefore, the analysis of the ratio of convective rainfall in this study is mainly based on the other subregions, and the ratio over the Tibetan Plateau will not be discussed hereafter, despite the fact that the values are listed in the following tables. The peaks and median ratio indicate that thunderstorms over the hilly land have the largest ratio of convective rainfall, followed by the foothills. Thunderstorms over the ocean have more stratiform precipitation compared with the continental regions. More than half of the continental thunderstorms contain more than 80% (refer to 0.8 in the Fig. 3) convective precipitation; this percentage over the ocean is about 70%. The variation in the

Atmos. Chem. Phys. Discuss., https://doi.org/10.5194/acp-2018-778
Manuscript under review for journal Atmos. Chem. Phys.
Discussion started: 28 August 2018

convective rainfall ratio shows that thunderstorms are mainly dominated by convective precipitation, while only a small number of thunderstorms have less convective precipitation, which are considered to be the thunderstorms at later stage or even dissipation stage. This will be further discussed in detail later.

Furthermore, based on the convective rainfall ratio at different grades, the PR vertical and horizontal characteristics of both thunderstorms and non-thunderstorms over different subregions (Table 2) are investigated. All the results consistently indicate that thunderstorms are significantly taller in height and larger in horizontal scale compared with those precipitation events without lightning, regardless of the ratio, echo intensity, or subregion. Most thunderstorms have a convective rainfall ratio greater than 0.75, and the population of thunderstorms decreases significantly as the ratio values decrease. This trend is particularly evident in the hilly land and foothills. There is still a small number of thunderstorms dominated by stratiform rainfall, with the ratio less than 0.25, which will be discussed in the following section. With the decrease in convective rainfall ratio, the maximum 20, 30, and 40 dBZ echo top heights of both thunderstorms and non-thunderstorms decrease; the weak echo horizontal scales are consistently increasing while the strong echo horizontal scale shows a different feature, which increases first and then decreases. Among the four subregions, the different echo horizontal scales of both thunderstorms and non-thunderstorms all consistently increase from west to east irrespective of the convective rainfall ratio. Following the view that the ratio of convective precipitation decreases gradually with the development and evolution of convective system, the

Atmos. Chem. Phys. Discuss., https://doi.org/10.5194/acp-2018-778
Manuscript under review for journal Atmos. Chem. Phys.
Discussion started: 28 August 2018

statistical results reveal that thunderstorms in the earlier stage are taller in vertical profile and smaller in horizontal scale compared with the later stages of thunderstorms. It should be noted that thunderstorms with convective rainfall ratio greater than or equal to 0.75 are tallest over the hilly land, followed by the foothills, and then the ocean. However, thunderstorms with a ratio less than 0.75 show a different pattern: the echo top height decreases from the ocean to the hilly land and then to the foothills. For non-thunderstorms, their echo top heights decrease from west to east always.

As can be seen from the results of Table 2 and Fig. 3, although most of the thunderstorms are dominated by convective precipitation, there is still a small amount of thunderstorms that coexist with wide stratiform rainfall, or are even dominated by stratiform precipitation. Therefore, such weak thunderstorms (precipitation events with lightning but the maximum PR reflectivity is less than 40 dBZ) and strong convective events (precipitation events with maximum PR reflectivity reaches or exceeds 40 dBZ while regardless of lightning) are further compared. The statistical results in table 3 indicate that although there are indeed some weak thunderstorms, their occurrence frequency over the three lower subregions is actually much lower than that of strong convective events. In contrast, weak thunderstorms over the Tibetan Plateau occur frequently, and the number is comparable to that of strong convective events. This further shows the particularity of the plateau thunderstorms, which is worth more attention in future work. The 20 dBZ, 30 dBZ and 40 dBZ radar echo pixels counts reveal that the horizontal scale of weak thunderstorms is distinctly smaller than that of strong convective events in all subregions, even though they are accompanied by lightning. The PR echo top height also shows a similar characteristic: the vertical height of weak thunderstorms is lower than that of strong convective events over land regions. In contrast, over the ocean, the echo top heights of weak thunderstorms are taller than those of strong convective events. To clarify this characteristic, the vertical structure of strong convective events is further investigated: the results show that the 20 dBZ and 30 dBZ echo top heights of strong convective events without lightning are significantly lower than those with lightning and are also lower than those of weak thunderstorms. The percentage of strong convective events without lightning accounts for the total number of strong convective events being the largest over the ocean (~90%), obviously greater than the hilly land and foothills (~72%), which result in the echo top heights of strong convective events being lower than those of weak thunderstorms over the ocean. It should be noted that although the echo top heights of weaker reflectivity in such strong convective events are relatively low, their gaps between different echo top heights (MaxH20-MaxH30 and MaxH30-MaxH40) are smaller and the convective rainfall ratio is larger, which reveals that such strong convective events are in the earlier developing stage. The convective rainfall ratios of weak thunderstorms over the land regions are 0.33 over the plateau, 0.45 over the foothills, and 0.50 over hilly land, significantly less than the ratios of 0.65, 0.73, and 0.76 for strong convective events, respectively. Finally, integrating the above results together, it can be concluded that weak thunderstorms observed by TRMM satellite, in terms of smaller horizontal scale, lower echo top height, and less convective precipitation, should be mainly thunderstorms in a later stage or even the dissipation stage instead of isolated weak thunderstorms. This is because an isolated weak thunderstorm is not strong enough to produce lightning in such a weak convective intensity, with weak convective echo core (maximum reflectivity less than 40 dBZ) and small horizontal scale.

(Figure 3 and Tables 2 and 3)

3.3 Occurrence probability of lightning in strong convective events

The electrification and discharge processes in thunderstorm are closely related to the development and interaction of dynamic and microphysical processes. With the evolution and enhancement of convective cloud, the interaction of hydrometeors (such as ice crystal, hail, snow, and graupel) increases, and lightning discharge is produced when the electric field in thunderclouds break through a certain threshold. The stronger the convective intensity of a thunderstorm, the more the lightning. But, when a convective system produces lightning is still a scientific issue. Therefore, this section further investigates the occurrence probability of lightning in strong convective events as discussed in the previous section (refer to table 3).

The convective intensity can be defined by the properties of the convective updrafts in a storm (Zipser et al., 2006), but it is difficult to measure them, especially over large areas and for long periods. According to the characteristics of convection, more vigorous convective updraft means stronger convective intensity, which brings more and larger precipitation particles to higher altitudes, leading to a higher echo top height. Therefore, the echo top height is adopted as an alternative to convective

Atmos. Chem. Phys. Discuss., https://doi.org/10.5194/acp-2018-778
Manuscript under review for journal Atmos. Chem. Phys.
Discussion started: 28 August 2018

intensity. The occurrence probability of lightning in strong convective events as a function of the maximum 20, 30, and 40 dBZ echo top heights over different subregions are shown in Figures 4 and 5. It can be seen that the occurrence probability of lightning in strong convective events over the foothills and hilly land is significantly larger than that over the plateau and ocean. Owing to the higher elevation of the Tibetan Plateau, even though the echo top height of convection is similar to that of the other subregions, the probability of lightning is significantly lower than in the other subregions, even lower than that for the ocean. Of course, this phenomenon is also partly caused by thunderstorm itself being weaker over the Tibetan Plateau with such an echo top height due to its higher elevation. The convection distribution according to the maximum 20, 30, and 40 dBZ echo top heights indicates that convection over the ocean is mainly characterized by lower echo top heights, and the number of strong convective events with higher echo top heights (e.g., maximum 30 dBZ echo height exceeding 10 km) is significantly less compared with the other regions.

Comparing the relationship between lightning probability and maximum echo top heights of different radar reflectivity in Figures 4 and 5, it can be seen that the maximum 30 dBZ echo top height shows a simpler and more intuitive characteristic compared with the 20 and 40 dBZ echo top heights. This is particularly significant over the foothills and hilly land. Strong convective events with a 30 dBZ echo top height less than 5 km altitude do not have any flashes basically. The occurrence probability of lightning in strong convective events with a 30 dBZ echo top height between 5 km and 7 km is small, less than 40%. The probability value increases with increasing 30 dBZ echo top height. It is between 40% and 70% when the maximum 30 dBZ echo height of convection is in the range of 7–9 km, and when the height exceeds 9 km, the probability exceeds 80%. The relationship over the ocean shows a similar pattern with that over the foothills and hilly land; the main difference is the smaller probability values relative to the same reference height. In contrast, the relationship between lightning probability and the maximum echo top heights of 20 and 40 dBZ are more complex and confusing. For example, the occurrence probability of lightning in strong convective events with 20 dBZ (40 dBZ) echo top height at 12 km (5 km) altitude shows a very wide range, covering almost all probabilities from zero to 100%. Over the Tibetan Plateau, the occurrence probability of lightning in strong convective events is the lowest, with almost no probabilities more than 90%, and the relationship with the 30 dBZ echo top height is also weaker compared with the other subregions.

Although the lightning activity has a good correlation with the convective intensity of the convective storm, there are still many issues that need further clarification. The probability of lightning in a strong convective event with a maximum 30 dBZ echo top height exceeding 9 km altitude is not 100%, which means that there are some strong convective events do not have lightning observed by the LIS. Why? This study further calculates some statistical parameters (the count, maximum pixels of 30 dBZ echo and ratio of convective rainfall to total rainfall) for strong convective events with and without lightning based on the different maximum

Atmos. Chem. Phys. Discuss., https://doi.org/10.5194/acp-2018-778
Manuscript under review for journal Atmos. Chem. Phys.
Discussion started: 28 August 2018

30 dBZ echo top heights and the results are shown in Table 4. From the values listed in Table 4, it can be seen that with increasing 30 dBZ echo top height, the count (or percentage) of strong convective events with lightning over the four subregions consistently increase. However, the variation in the count of strong convective events without lightning over the different subregions shows a different pattern. The count increases over the Tibetan Plateau while it decreases over the ocean. In the two low-altitude land regions, the count of strong convective events without lightning is largest when the 30 dBZ echo top height is between 5 and 7 km. The horizontal scale (30 dBZ) of strong convective events with lightning is significantly larger than that of strong convective events without lightning, regardless of subregion or 30 dBZ echo top heights. A comparison of the horizontal scale and ratio of convective rainfall to total rainfall of strong convective events with and without lightning shows that strong convective events without lightning are significantly smaller in horizontal scale and slightly larger in the ratio of convective rainfall compared with those with lightning. The result clearly indicates that, in the case of similar radar echo top heights, strong convective events without lightning may be in the pre-lightning stage or the earlier developing stage of thunderstorms compare to those with lightning. They will probably produce lightning if their convective intensities further enhance. It should be noted that although it should be rare, there still be some cases where lightning was not seen by the LIS but in fact occurred in practise.

(Figures 4 and 5, and Table 4.)

Atmos. Chem. Phys. Discuss., https://doi.org/10.5194/acp-2018-778
Manuscript under review for journal Atmos. Chem. Phys.
Discussion started: 28 August 2018

3.4 The most intense thunderstorms

The stronger the convective intensity of a thunderstorm, the higher the height attained by the strong echo top (40 dBZ) and the larger the lightning flash rate. As a result, more serious loss and damage will be caused, and the vertical upward transport of water vapor and pollutants into the upper troposphere/lower stratosphere will be more considerable. Therefore, in order to improve the understanding of the most intense thunderstorms, the characteristics of lightning and dynamic processes with evolution of the most intense thunderstorms over foothills and hilly land are further investigated in this section. The most intense thunderstorms here refer to the top 0.1% of convective parameters in Zipser et al. (2006), that is maximum 40 dBZ echo height exceeding 10.5 km or lightning flash rate greater than 32 fl min^{-1}. Thunderstorms are divided into three types according to the two thresholds: storm-A-type thunderstorms are defined as those with a maximum 40 dBZ echo height exceeding 10.5 km while with a lightning flash rate less than 32 fl min^{-1}; storm-B-type thunderstorms are defined as those with both thresholds attained; and storm-C-type thunderstorms are defined as those with a maximum 40 dBZ echo height lower than 10.5 km but with a lightning flash rate greater than 32 fl min^{-1}. Statistical parameter values for the three types of thunderstorms are listed in Table 5. The lightning flash rate together with the maximum 20, 30, and 40 dBZ echo top heights indicate that the convective intensity of storm-B-type is the most intense among the three types of thunderstorms, while the horizontal scale of thunderstorms (refer to the radar echo pixels of 20, 30, and 40 dBZ pixels), shows that storm-C-type is the largest and storm-A-type is the smallest. The ratio of convective rainfall to total rainfall of storm-A-type is the largest (0.9), followed by 0.85 for storm-B-type, and storm-C-type is the smallest (0.74). In addition, the vertical spacing between the top height of different echoes (20 versus 30 dBZ and 30 versus 40 dBZ) of storm-A-type is the smallest, followed by storm-B-type, and finally storm-C-type. The smaller vertical gaps between the top height of different echoes means the thundercloud top structure is more compact, and vice versa. Considering all these features together, the results indicate that storm-B-type is the most intense among the three types of thunderstorms, with the tallest echo top heights and the most frequent lightning activity. The three types of convective storm are in different life cycle stages of thunderstorms according to their convective properties. Storm-A-type, in terms of lower echo top heights, smaller horizontal scale, lower lightning flash rate, but more compact cloud top structure, is considered to be the pre-mature stage, younger or in an earlier stage compared with the mature stage of storm-B-type. Conversely, storm-C-type is considered to be the post-mature stage, which is older or in a later stage than the mature stage, with a larger horizontal scale, less convective rainfall and more fluffy cloud top structure. This result further confirms that using the convective rainfall ratio together with the radar echo structures to identify the stage of thunderstorms is an effective method to analysis the convective events observed by non-geostationary orbit satellites.

(Table 5)

4 Lightning and echo structure patterns of thunderstorms

It is generally considered that the electrical process and the dynamic process are closely related in a thundercloud: the stronger the convective intensity of a thunderstorm, the greater the accompanying lightning flash rate. However, the statistical results in this study show that this is not the case in different stages of thunderstorms. But no matter what, for those intense thunderstorms, they must go through a life cycle processes from the initial trigger to the mature stage and finally their dissipation. Based on the comparative analysis of the lightning flash rate, radar echo structure characteristics and the convective rainfall ratio of thunderstorms from the LIS and the PR onboard the TRMM satellite, it can be concluded that the lightning activity lags behind the development of radar echo structure with the evolution of thunderstorm.

A schematic diagram illustrating the coupling patterns of the radar echo structure feature and lightning activity in different evolution stages of the thunderstorm life cycle is shown in figure 6. In the cumulus stage (or initial developing stage) of thunderstorms, the convective cloud is energetic and dominated by strong updraft, when the horizontal scale is small but its vertical structure is thriving, with a strong radar echo core (over 40 dBZ) and dense cloud top structure. Nevertheless, the convective cloud at this stage is not or not yet strong enough to generate lightning. This is the main reason why some convective systems observed by the TRMM satellite have strong radar echo but no lightning. In fact, convective systems of this kind are usually in the rapid development and enhancement stage. They will soon develop and evolve into a mature stage of thunderstorm, characterized by high echo top height, strong radar echo core and active lightning discharge. This also means that thunderstorms are in the most powerful and the most destructive stage with both the most active electrical discharge process and the most robust dynamic process, which not only produces damage on the ground but also transports water particles to upper troposphere or even penetrates the tropopause and directly enter the stratosphere. Note that downdrafts caused by the drag effect of rainfall are also increasing during this period. Then after, as the unstable energy is consumed, the updraft is weakened while the downdraft is enhanced and begins to become dominant. As a result, the lightning flash rate and the ratio of convective rainfall to total rainfall begin to decrease. In the dissipation stage of a thunderstorm, the thundercloud collapses and dissipates rapidly without the support of the updraft, the radar echo top height decreases, and the stronger radar echo weakens more rapidly. As shown in Fig. 6, the intense echo core weakens significantly, its maximum reflectivity is less than 40 dBZ and the echo top structure in this stage is significantly less well organized than in the previous stages, with larger spacing between the different radar echo tops. From the perspective of vertical radar echo top heights and radar echo core, it reveals that convective intensity of thunderstorms in this stage are significantly weaker than that in the cumulus stage. The stratiform rainfall is dominant during this period while in the cumulus stage it is dominated by convective rainfall. Nonetheless, there is still a small amount of lightning discharges as can be seen by the LIS in this stage. This mainly results from charge transported from the upper to lower regions of cloud by downdrafts, which can enhance the electric field stress in and below the cloud base and further produce lightning discharge, although the charge generating mechanisms in cloud have ceased without the support of updrafts in the dissipation stage (Pawar and Kamra, 2013). Therefore, some storms have lightning where the radar echo core is especially weak with maximum radar reflectivity less than 40 dBZ. Ultimately, the thunderstorm goes through the dissipating stage, breaking and dissipating quickly without the support of the updraft.

More specifically, according to different patterns of convective parameters, such as echo top heights and lightning flash rate, the mature stage of thunderstorms can be further finely divided into three stages: 1) the pre-mature stage; 2) the mature stage; and 3) the post-mature stage, illustrating the evolutionary characteristics of electrical and dynamic processes with the evolution of thunderstorms. Here, the mature stage refers in particularly the most intense stage of thunderstorms, its most typical feature is that the updraft reaches the highest altitude. Thunderstorms at this stage have the largest lightning flash rate, the most intense radar echo core and the highest echo top heights. Correspondingly, in the pre-mature stage thunderstorm, all the convective parameters of echo top height, lightning flash rate and horizontal scale are in a rapid development and enhancement. The horizontal scale of thunderstorms in this stage is still small, dominated by upward motion despite the downdraft also being intensified compared to the previous stage. Dangerous weather phenomenon, such as lightning jump, hailfall and strong wind, are most likely to appear at this stage. However, the results from table 5 show that the lightning flash rate in this stage is significantly less than in the mature stage, and even in the post-mature stage. In the post-mature stage, the updraft weaken and the downdraft continues to increase and gradually begins to dominate. As a result, echo top height, lightning activity and convective rainfall begin to decrease but the horizontal scale, to a certain extent, still increases. Note that, although the lightning flash rate in this stage has decreased, it is still larger than that in the pre-mature stage, with the similar vertical echo top heights. After this, the thunderstorm is controlled by the downdraft and begins to enter the dissipating stage as mentioned in the previous paragraph.

(Figure 6)

5 Conclusions and discussion

In this study, thunderstorms over different terrain conditions in subtropical East Asia, from the Tibetan Plateau, east to the adjacent foothills, hilly land, and finally the coastal ocean, has been investigated using 16-year data from the TRMM satellite. Convective parameters of lightning activity and radar structure characteristics with the development and evolution of thunderstorms are statistical analyzed. The major findings are summarized as follows:

The occurrence frequency of thunderstorms over the different terrain conditions shows significant differences. The occurrence of thunderstorms over the Tibetan Plateau is the most frequent, accounting for about 20% of the total precipitation events observed by the TRMM PR, followed by the ~10% over foothills and hilly land. But, the convective intensity of thunderstorms over the hilly land is the most intense, followed by the foothills, and weakest over the Tibetan Plateau despite the occurrence of thunderstorms being the most frequent there. The occurrence of thunderstorms over the ocean is the least, while their horizontal scale is larger than that over land and their convective intensity is greater than that over the Tibetan Plateau. Both the horizontal scale and vertical height of thunderstorms are always significantly greater than those convective events without lightning.

It is well known that the lightning flash rate and intense radar echo top height are closely related to the convective intensity of thunderstorms: the stronger the convective intensity, the larger the lightning flash rate and the higher the echo top height. Nevertheless, the present study indicates that the coupling patterns of lightning and echo top heights of thunderstorms are different in different life cycle stages of thunderstorms. This will cause some negative effects when considering convective intensity or analyzing the correlation between lightning flash rate and radar echo top heights of thunderstorms, especially for those observed by non-geostationary orbit satellites. This study confirms that, combining the ratio of convective rainfall to total rainfall with the three-dimension radar echo structure of convective event provides be a valuable method to distinguish the stage of different thunderstorm fragments. Those strong convective events with a maximum radar reflectivity exceeding 40 dBZ but no lightning, are identified as thunderstorms in the initial developing/cumulus stage according to characteristics of more convective rainfall, smaller horizontal scale, and more compact cloud top structure. In contrast, those weak thunderstorms with lightning but especially weak radar echo core (maximum reflectivity less than 40 dBZ) in terms of less convective precipitation, lower echo top height, and larger vertical spacing between different echo tops illustrate that they are actually thunderstorms in the dissipating stage.

In order to explore when a convective event can produce lightning, this study further investigated the occurrence probability of lightning in strong convective events with different convective intensity. The results reveal that for those strong convective events with maximum reflectivity exceeding 40 dBZ, the maximum 30 dBZ echo top height shows a more concise relationship with the occurrence probability of lightning in strong convective storms compared with the maximum 20 and 40 dBZ echo top heights. When the maximum 30 dBZ echo top height of strong convective events exceeds 9 km, the occurrence probability of lightning exceeds 80%. When the maximum 30 dBZ echo top height is in the range of 7-9 km, the probability is between 40% and 70 %. Almost no lightning occurs in strong convective events with a 30 dBZ echo top height lower than 5 km altitude. The result is of great significance for the probability forecast of lightning in strong convective storms, which will be very useful for lightning nowcasting and warning services. Those strong convective events with a similar 30 dBZ echo top height but no lightning, which are characterized by smaller horizontal scale and more convective rainfall, are considered to be thunderstorms in an earlier stage compared with those with lightning.

Based on statistical and comparative analysis from the 16-year TRMM satellite data, this study further summarizes the patterns of lightning activity and dynamic processes with the evolution of thunderstorms. The results indicate that the evolution of lightning activity lags behind the development of vertical radar echo structure during the entire life cycles of thunderstorms. When a thunderstorm is in the mature stage, its convective intensity parameters such as lightning flash rate and strong radar echo top heights all reach their peak levels. But, before a thunderstorm reaches its mature stage, it is dominated by updraft and shows energetic convective developing features in terms of larger convective rainfall ratio, smaller horizontal scale but stronger radar echo core and more compact cloud top structure. Conversely, when a thunderstorm has gone through its mature stage, it is dominated by downdrafts and appears to be weak in radar echo structure, featuring a larger horizontal scale, less convective rainfall ratio, and more fluffy cloud top structure. Furthermore, for some thunderstorms in the developing stage, although the radar echo top can reach a higher altitude, there may still be no lightning. Conversely, thunderstorms that are in the dissipating stage, although the convective intensity has been significantly weakened, may still have lightning.

The non-geostationary-orbit satellites (i.e., the TRMM, the GPM and so on) have provided plenty of valuable observational data for studying the climatic characteristics of precipitation and convective systems over larger areas and even global scale over a long period. The present study has demonstrated that using the ratio of convective rainfall to total rainfall together with the radar echo top structure to identify the evolution stage of thunderstorms is a useful method for analyzing the TRMM data. This method should be a valuable reference in analyzing time discontinuous observation data provided by non-geostationary-orbit satellites or some ground-based instruments. It can help us further explore and maximize the use of those valuable observation data. In addition, in some cases, only the edge portion of convective storms are observed by satellites as the convective core is located outside of the scanning range, which can more or less adversely affect the results of statistical analysis and should be paid more attention in future studies.

Acknowledgment: The authors gratefully acknowledge the University of Utah for providing the TRMM database via their website (http://trmm.chpc.utah.edu/). This research was supported jointly by the National Natural Science Foundation of China (41605001), the National Key Basic Research and Development (973) Program of China (2014CB441406) and the Fundamental Research Funds for the Central Universities lzujbky-2015-12.

References

Albrecht, R. I., Goodman, S. J., Buechler, D. E., Blakeslee, R. J., and Christian, H. J. J.: Where are the lightning hotspots on Earth? Bull. Amer. Meteor. Soc. 97, 2051-2068, doi:10.1175/BAMS-D-14-00193.1, 2016.

Bang, S. D., and Zipser, E. J.: Differences in size spectra of electrified storms over land and ocean, Geophys. Res. Lett., 42, 6844 – 6851, doi:10.1002/2015GL065264, 2015.

Bürgesser, R. E., Pereyra, R. G., and Avila, E. E.: Charge separation in updraft of convective regions of thunderstorm, Geophys. Res. Lett., 33, L03808, doi:10.1029/2005GL023993, 2006.

Cecil, D. J., Buechler, D. E., and Blakeslee, R. J.: Gridded lightning climatology from TRMM-LIS and OTD: Dataset description, Atmos. Res., doi:10.1016/j.atmosres.2012.06.028, 2014.

Atmos. Chem. Phys. Discuss., https://doi.org/10.5194/acp-2018-778
Manuscript under review for journal Atmos. Chem. Phys.
Discussion started: 28 August 2018

Cecil, D. J., Goodman, S. J., Boccippio, D. J., Zipser, E. J., and Nesbitt, S. W.: Three years of TRMM precipitation features. Part I: Radar, radiometric, and lightning characteristics, Mon. Weather Rev., 133, 543 – 566, 2005.

Deierling, W., and Petersen, W. A.: Total lightning activity as an indicator of updraft characteristics, J. Geophys. Res., 113, 280-288, 2008.

Fierro, A. O., Gao, J., Ziegler, C. L., Mansell, E. R., Macgorman, D. R., and Dembek, S. R.: Evaluation of a Cloud-Scale Lightning Data Assimilation Technique and a 3DVAR Method for the Analysis and Short-Term Forecast of the 29 June 2012 Derecho Event, Mon. Weather Rev., 142, 183-202, 2013.

Fu, Y. and Liu, G.: Possible Misidentification of Rain Type by TRMM PR over Tibetan Plateau, J. Appl. Meteor. Climatol., 46, 667-672, 2007.

Houze, R. A.: Stratiform precipitation in regions of convection: a meteorological paradox? Bull. Amer. Meteor. Soc., 78, 2179-2196, 1997.

Houze, R. A., Wilton, D. C., and Smull, B. F.: Monsoon convection in the Himalayan region as seen by the TRMM Precipitation Radar, Quart. J. Roy. Meteor. Soc., 133, 1389-1411, 2007.

Houze, R. A., Rasmussen, K. L., Zuluaga, M. D., and Brodzik, S. R.: The variable nature of convection in the tropics and subtropics: A legacy of 16 years of the Tropical Rainfall Measuring Mission satellite, Rev. Geophys., 53, doi:10.1002/2015RG000488, 2015.

Iguchi, T., Kozu, T., Meneghini, R., Awaka, J. and Okamoto, K.: Rain-profiling algorithm for the TRMM precipitation radar. J. Appl. Meteor., 39, 2038-2052, 2000.

Ingersoll, A. P., Gierasch, P. J., Banfield, D., Vasavada, A. R., and Galileo Imaging Team.: Moist convection as an energy source for the large-scale motions in Jupiter's atmosphere, Nature, 403, 630-632, 2000.

Iordanidou, V., Koutroulis, A. G., and Tsanis, I. K.: Investigating the relationship of lightning activity and rainfall: A case study for Crete Island, Atmos. Res., 172, 16-27, 2016.

Jayaratne, E. R., Saunders, C. P. R., and Hallett, J.: Laboratory studies of the charging of soft hail during ice crystals interactions, Q. J. R. Meteorol. Soc., 109, 609 – 630, 1983.

Kummerow, C., Simpson, J., Thiele, O., Barnes, W., Chang, A. T. C., Stocker, E., Adler, R. F., Hou, A., Kakar, R., Wentz, F., Ashcroft, P., Kozu, T., Hong, Y., Okamoto, K., Iguchi, T., Kuroiwa, H., Im, E., Haddad, Z., Huffman, G., Ferrier, B., Olson, W. S., Zipser, E., Smith, E. A., Wilheit, T. T., North, G., Krishnamurti, T., and Nakamura, K.: The status of the Tropical Rainfall Measuring Mission (TRMM) after two years in orbit, J. Appl. Meteor., 39, 1965 – 1982, 2000.

Kummerow, C., Barnes, W., Kozu, T., Shiue, J., and Simpson, J.: The tropical rainfall measuring mission (TRMM) sensor package, J. Atmos. Oceanic Technol., 15, 809-817, 1998.

Liu, C. T., Zipser, E. J., Cecil, D. J., Nesbitt, S. W., and Sherwood, S.: A cloud and precipitation feature database from nine years of TRMM observations, J. Appl. Meteor. Climatol., **47**, 2712-2728, 2008.

Liu, C., and Zipser, E. J.: Global distribution of convection penetrating the tropical tropopause, J. Geophys. Res., 110, D23104, doi:10.1029/2005JD006063, 2005.

Liu, C., Cecil, D. J., Zipser, E. J., Kronfeld, K., and Robertson, R.: Relationships between lightning flash rates and radar reflectivity vertical structures in thunderstorms over the tropics and subtropics, J. Geophys. Res., **117**, D06212, doi:10.1029/2011JD017123, 2012.

Liu, C., Zipser, E. J., and Nesbitt, S. W.: Global Distribution of Tropical Deep Convection:

Different Perspectives from TRMM Infrared and Radar Data, J. Climate, 20, 489 – 503.doi: http://dx.doi.org/10.1175/JCLI4023.1, 2007.

Luo, Y. L., Zhang, R., Qian, W., Luo, Z., and Hu, X.: Intercomparison of deep convection over the Tibetan Plateau-Asian monsoon region and subtropical North America in boreal summer using CloudSat/CALIPSO data, J. Climate, **24**, 2164-2177, 2011.

Mansell, E. R., Ziegler, C. L., and Macgorman, D R.: A Lightning Data Assimilation Technique for Mesoscale Forecast Models, Mon. Weather Rev., 135, 1732-1748, 2007.

Nesbitt, S. W., Zipser, E. J., and Cecil, D. J.: A census of precipitation features in the tropics using TRMM: Radar, ice scattering, and lightning observations, J. Climate, 13, 4087 – 4106, 2000.

Park, M., Randel, W. J., Gettelman, A., Massie, S. T., and Jiang, J. H.: Transport above the Asian summer monsoon anticyclone inferred from Aura Microwave Limb Sounder tracers, J. Geophys. Res., 112, D16309, doi:10.1029/2006JD008294, 2007.

Pessi, A. T., and Businger, S.: Relationships among lightning, precipitation, and hydrometeor characteristics over the North Pacific Ocean, J. Appl. Meteorol. Climatol., 48, 833 – 848, doi:10.1175/2008JAMC1817.1, 2009.

Petersen W A and Rutledge, S A.: On the relationship between cloud-to-ground lightning and convective rainfall, J. Geophys. Res., 103(D12):14025-14040, 1998.

Petersen, W. A., Christian, H. J., and Rutledge, S. A.: TRMM observations of the global relationship between ice water content and lightning, Geophys. Res. Lett., 32, L14819, doi:10.1029/2005GL023236, 2005.

Qie, X., Zhang, Y., Yuan, T., Zhang, Q., Zhang, T., Zhu, B., Lü, W., Ma, M., Yang, J., Zhou, Y., and Feng, G.: A review of atmospheric electricity research in China, Adv. Atmos. Sci., 32: 169

– 191, doi: 10.1007/s00376-014-0003-z, 2015.

Qie, X., Wu, X., Yuan, T., Bian, J., and Lu, D.: Comprehensive Pattern of Deep Convective Systems over the Tibetan Plateau – South Asian Monsoon Region Based on TRMM Data, J. Climate, 27, 6612 – 6626. doi: http://dx.doi.org/10.1175/JCLI-D-14-00076.1, 2014.

Qie, X., Zhu, R., Yuan, T., Wu, X., Li, W., and Liu, D.: Application of total-lightning data assimilation in a mesoscale convective system based on the WRF model, Atmos. Res., s145 – 146, 255-266, 2014.

Randel, W. J., Park, M., Emmons, L., Kinnison, D., Bernath, P., Walker, K. A., Boone, C., and Pumphrey, H.: Asian monsoon transport of pollution to the stratosphere, Science, 328, 611-613, doi:10.1126/science.1182274, 2010.

Rasmussen, K. L., Zuluaga, M. D., and Houze, R. A.: Severe convection and lightning in subtropical South America, Geophys. Res. Lett., 41, 7359 – 7366, doi:10.1002/2014GL061767, 2014.

Reynolds, S. E., Brook, M., and Gourley, M. F.: Thunderstorm charge separation, J. Meteorol., 14, 426– 436, 1957.

Romatschke, U., Medina, S., and Houze, R. A.: Regional, seasonal, and diurnal variations of extreme convection in the South Asian region, J. Climate, 23, 419-439, 2010.

Saunders, C. P. R., Keith, W. D., and Mitzeva, R. P.: The effect of liquid water on thunderstorm charging, J. Geophys. Res., 96, 11007 – 11017, 1991.

Takahashi, T.: Riming electrification as a charge generation mechanism in thunderstorms, J. Atmos. Sci., 35, 1536 – 1548, 1978.

Takayabu, Y. N.: Rain-yield per flash calculated from TRMM PR and LIS data and its relationship

Atmos. Chem. Phys. Discuss., https://doi.org/10.5194/acp-2018-778
Manuscript under review for journal Atmos. Chem. Phys.
Discussion started: 28 August 2018

to the contribution of tall convective rain, Geophys. Res. Lett., 33, 510-527, 2006.

Toracinta, E. R., Cecil, D. J., Zipser, E. J., and Nesbitt, S. W.: Radar, Passive Microwave, and Lightning Characteristics of Precipitating Systems in the Tropics, Mon. Weather Rev., 130, 802-824, 2002.

Ushio, T., Heckman, S. J., Boccippio, D. J., Christian, H. J., and Kawasaki, Z.-I.: A survey of thunderstorm flash rates compared to cloud top height using TRMM satellite data, J. Geophys. Res., 106, 24,089–24,095, doi:10.1029/2001JD900233, 2001.

Wu, X., Qie, X., Yuan, T., and Li, J.: Meteorological regimes of the most intense convective systems along the southern Himalayan front, J. Climate, 29, 4383-4398, 2016.

Zheng, D., Zhang, Y., Meng, Q., Chen, L., and Dan, J.: Climatology of lightning activity in South China and its relationships to precipitation and convective available potential energy, Adv. Atmos. Sci., 33, 365-376, 2016.

Zipser, E. J., Cecil, D. J., Liu, C. T., Nesbitt, S. W., and Yorty, D. P.: Where are the most intense thunderstorms on earth? Bull. Amer. Meteor. Soc., 87, 1057-1071, 2006.

Zuluaga, M., and Houze, R. A.: Extreme convection of the near-equatorial Americas, Africa, and adjoining oceans as seen by TRMM, *Mon. Weather Rev.*, **143**, 298–316, 2015.

Atmos. Chem. Phys. Discuss., https://doi.org/10.5194/acp-2018-778
Manuscript under review for journal Atmos. Chem. Phys.
Discussion started: 28 August 2018

Figures and Tables

Figure 1

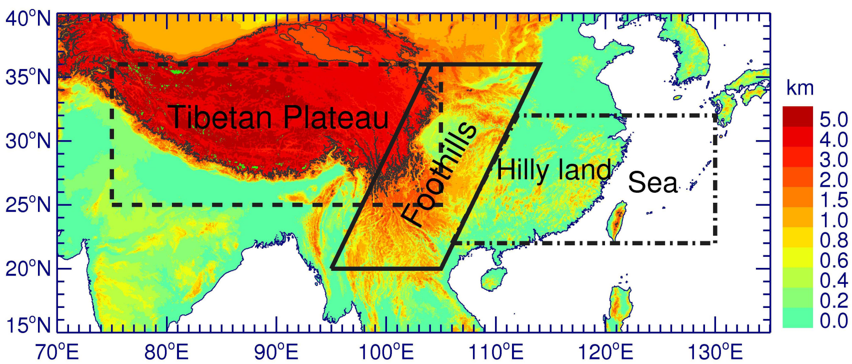

Figure 1 Location and geographic elevation of the four subregions in this study. The Tibetan Plateau is the area in the dashed box, with elevation greater than 3000 m. The foothills is the area in the solid box, with elevation lower than 3000 m. The hilly land is the continental area in the dash dot box and the sea is the oceanic area in the dash dot box. RPFs over islands are excluded in this study.

Figure 2

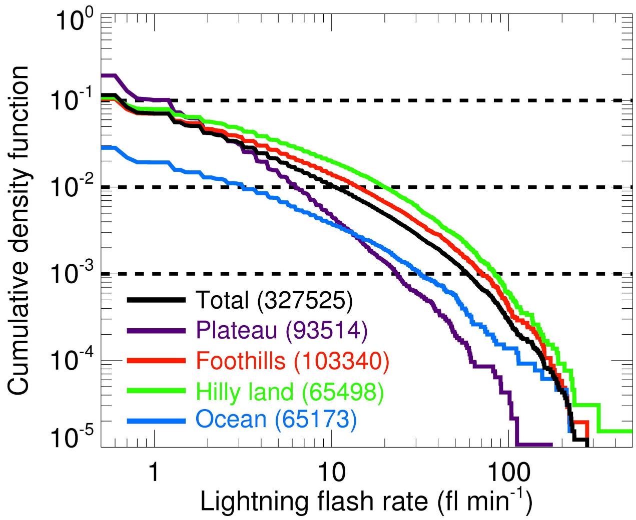

Figure 2. Cumulative distribution function (CDF) for lightning flash rate of RPFs over the four different subregions. Sample size is given in parentheses.

Atmos. Chem. Phys. Discuss., https://doi.org/10.5194/acp-2018-778
Manuscript under review for journal Atmos. Chem. Phys.
Discussion started: 28 August 2018

Figure 3

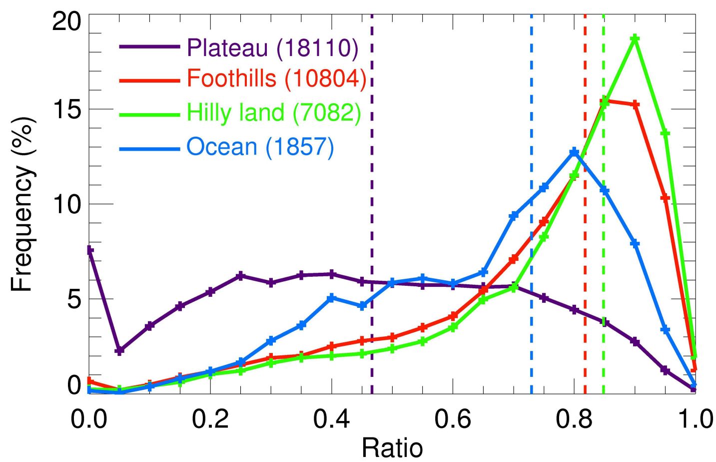

Figure 3 Frequency distribution of the ratio of convective rainfall to total rainfall of RPFs with lightning (thunderstorms) over the four different subregions. Sample size is given in parentheses and dashed lines represent the median ratio.

Atmos. Chem. Phys. Discuss., https://doi.org/10.5194/acp-2018-778
Manuscript under review for journal Atmos. Chem. Phys.
Discussion started: 28 August 2018

Figure 4

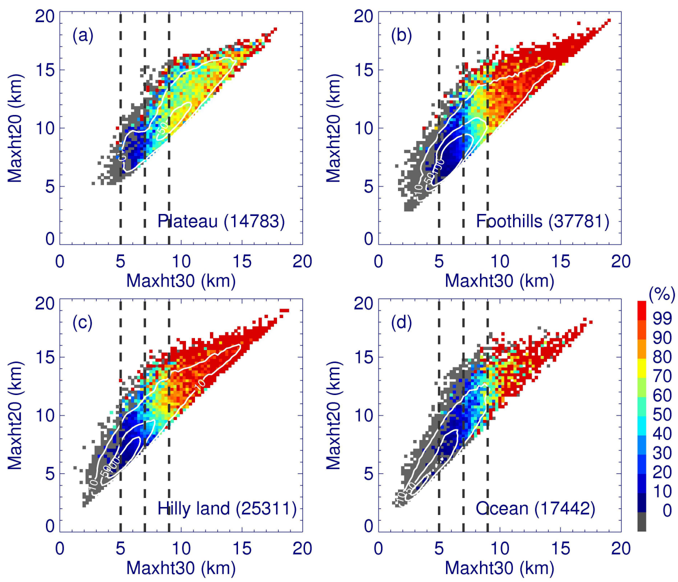

Figure 4. Occurrence probability of lightning in strong convective events with different 20 and 30 dBZ echo top heights over the (a) plateau, (b) foothills, (c) hilly land, and (d) ocean. White contours show the sample density of strong convective events.

Atmos. Chem. Phys. Discuss., https://doi.org/10.5194/acp-2018-778
Manuscript under review for journal Atmos. Chem. Phys.
Discussion started: 28 August 2018

Figure 5

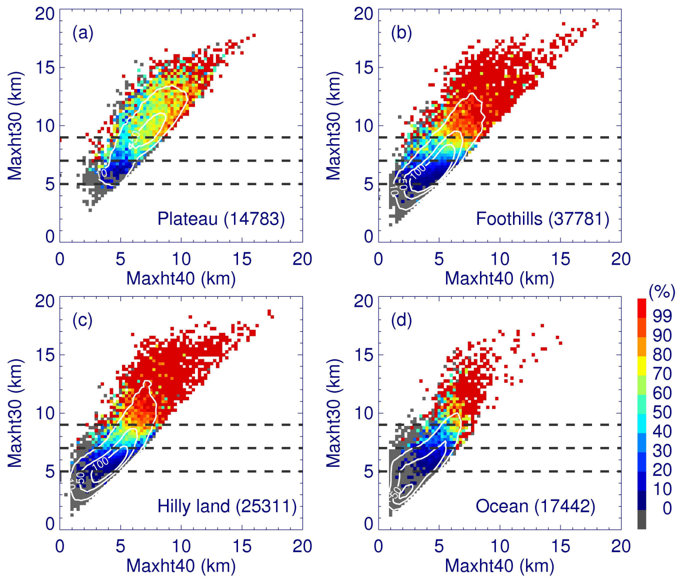

Figure 5. Same as Figure 4, but for 30 and 40 dBZ echo top heights.

Atmos. Chem. Phys. Discuss., https://doi.org/10.5194/acp-2018-778
Manuscript under review for journal Atmos. Chem. Phys.
Discussion started: 28 August 2018

Atmospheric Chemistry and Physics Discussions

Figure 6

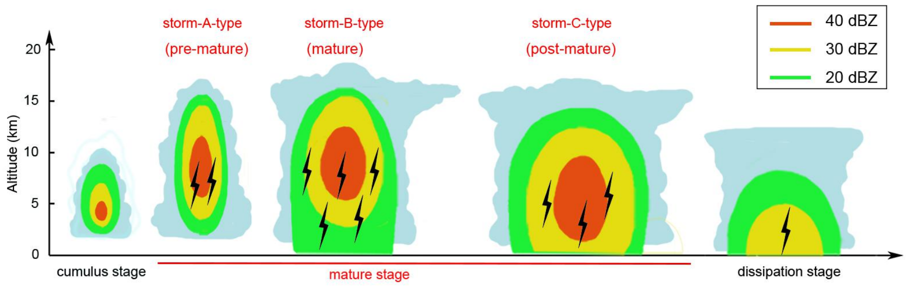

Figure 6. Schematic diagram of lightning activity and three-dimensional structural feature in several different stages of the thunderstorm lifecycle based on the TRMM satellite data. Light blue shades are cloud body profiles.

Atmos. Chem. Phys. Discuss., https://doi.org/10.5194/acp-2018-778
Manuscript under review for journal Atmos. Chem. Phys.
Discussion started: 28 August 2018

Table 1

Table 1 Statistical values of thunderstorms and non-thunderstorms over the four different subregions.

Subregion	Storm type	Count	Maximum height			Pixels number			Maximum Reflectivity
			20 dBZ	30 dBZ	40 dBZ	20 dBZ	30 dBZ	40 dBZ	
Plateau	Non-thunderstorm	75404	9.2	7.2	0.6	21.3	3.3	0.1	31.7
	Thunderstorm	18110	11.1	9.3	3.5	59.8	12.3	1.4	38.8
Foothills	Non-thunderstorm	92536	6.5	4.9	1.3	55.7	14.8	0.8	19.9
	Thunderstorm	10804	11.3	9.2	6.1	202.5	96.2	17.1	40.5
Hilly land	Non-thunderstorm	58416	5.8	4.2	1.2	71.4	19.9	1.2	14.1
	Thunderstorm	7082	11.9	9.6	6.4	297.1	151.1	28.0	41.0
Ocean	Non-thunderstorm	63316	5.1	3.6	0.8	70.0	22.4	1.8	10.1
	Thunderstorm	1857	11.8	9.2	5.9	659.8	349.2	62.6	39.9

Atmos. Chem. Phys. Discuss., https://doi.org/10.5194/acp-2018-778
Manuscript under review for journal Atmos. Chem. Phys.
Discussion started: 28 August 2018

Table 2

Table 2. Comparison of radar echo structure characteristics between thunderstorms and non-thunderstorms at different ratios of convective rainfall to total rainfall. The vertical and horizontal characteristics are shown by maximum echo top height and the maximum pixel number of 20, 30 and 40 dBZ, respectively.

Ratio		1.00~0.75		0.75~0.50		0.50~0.25		0.25~0.0	
lightning		Non-thunderstorm	Thunderstorm	Non-thunderstorm	Thunderstorm	Non-thunderstorm	Thunderstorm	Non-thunderstorm	Thunderstorm
Plateau	**Count**	**5125**	**3161**	**11760**	**5179**	**19975**	**5531**	**38544**	**4239**
	Maxht20/30/40	10.5/8.7/3.9	12.1/10.4/6.7	9.6/7.8/1.4	11.7/9.9/5.2	9.2/7.3/0.4	10.8/9.0/2.5	8.8/6.8/0.1	10.0/8.1/0.4
	N20/30/40	11/4/1	31/12/3	13/4/0	61/16/2	21/4/0	75/14/1	26/2/0	60/5/0
Foothills	**Count**	**26346**	**6786**	**16870**	**2493**	**14865**	**1159**	**34455**	**366**
	Maxht20/30/40	6.9/5.5/2.8	11.6/9.6/6.6	6.6/5.0/1.5	11.0/8.8/5.7	6.4/4.7/0.8	10.7/8.2/5.0	6.3/4.4/0.3	9.2/6.7/2.7
	N20/30/40	12/6/1	69/38/13	23/8/1	244/117/21	52/17/1	703/324/31	106/24/1	814/310/16
Hilly land	**Count**	**21418**	**4915**	**8947**	**1361**	**7056**	**628**	**20995**	**178**
	Maxht20/30/40	6.0/4.7/2.2	12.2/10.0/6.7	5.9/4.4/1.4	11.4/9.0/5.9	5.7/4.0/0.7	10.9/8.4/5.6	5.7/3.8/0.3	9.4/6.7/4.2
	N20/30/40	13/6/1	83/48/17	28/11/1	432/226/44	77/27/2	1341/654/76	147/36/1	1507/656/49
Ocean	**Count**	**31127**	**856**	**11009**	**623**	**7446**	**330**	**13734**	**48**
	MaxH20/30/40	4.6/3.4/1.0	11.8/9.4/5.9	5.8/4.1/1.1	12.1/9.3/6.0	5.4/3.7/0.8	11.6/8.7/5.8	5.4/3.6/0.3	10.1/7.0/4.9
	N20/30/40	14/6/1	148/85/26	45/18/2	684/371/74	139/56/6	1707/885/130	179/46/2	2283/1101/111

Atmos. Chem. Phys. Discuss., https://doi.org/10.5194/acp-2018-778
Manuscript under review for journal Atmos. Chem. Phys.
Discussion started: 28 August 2018

Atmospheric Chemistry and Physics
Discussions

Table 3

Table 3 Mean convective parameters of strong convective events (with maximum radar reflectivity exceeding 40 dBZ while regardless of lightning) and weak thunderstorms (with lightning but maximum radar reflectivity less than 40 dBZ) over the four different subregions.

		Count	Maximum height			Pixels count			Ratio
			20 dBZ	30 dBZ	40 dBZ	20 dBZ	30 dBZ	40 dBZ	
Plateau	Weak thunderstorm	10146	10.2	8.5	/	33	5	/	0.33
	Strong convection	14783	11.5	9.6	7.0	75	19	2	0.65
Foothills	Weak thunderstorm	595	8.3	6.4	/	36	6	/	0.45
	Strong convection	37781	8.8	6.9	4.9	143	56	7	0.73
Hilly land	Weak thunderstorm	115	7.7	5.0	/	27	8	/	0.50
	Strong convection	25311	8.5	6.7	4.5	191	79	11	0.76
Ocean	Weak thunderstorm	32	8.1	5.7	/	23	9	/	0.64
	Strong convection	17442	7.3	5.5	3.5	254	107	13	0.74

Atmos. Chem. Phys. Discuss., https://doi.org/10.5194/acp-2018-778
Manuscript under review for journal Atmos. Chem. Phys.
Discussion started: 28 August 2018

Table 4

Table 4 Count, average of the maximum 30 dBZ echo area (Area30) and ratio of convective rainfall to total rainfall (Ratio) of precipitation events for different 30 dBZ echo top height over the four subregions.

		0−5 km			5−7 km			7−9 km			9 km ~		
		count	Area30	Ratio	count	Area30	Ratio	count	Area30	Ratio	count	Area30	Ratio
Plateau	Non-thunderstorm	94	17	0.57	1719	30	0.55	1830	13	0.67	3176	8	0.72
	Thunderstorm	3	53	0.43	121	29	0.57	1542	19	0.60	6298	23	0.65
Foothills	Non-thunderstorm	3963	38	0.68	17659	40	0.71	5260	37	0.78	690	22	0.84
	Thunderstorm	33	52	0.59	1266	79	0.68	3802	84	0.75	5108	120	0.81
Hilly land	Non-thunderstorm	5509	49	0.74	9933	51	0.74	2536	60	0.81	366	40	0.86
	Thunderstorm	36	54	0.57	853	155	0.68	2254	162	0.76	3824	149	0.83
Ocean	Non-thunderstorm	7167	37	0.79	6429	95	0.70	1738	165	0.71	283	196	0.72
	Thunderstorm	11	102	0.57	226	210	0.64	686	341	0.67	902	406	0.70

Atmos. Chem. Phys. Discuss., https://doi.org/10.5194/acp-2018-778
Manuscript under review for journal Atmos. Chem. Phys.
Discussion started: 28 August 2018

Table 5

Table 5. Statistical characteristics of the most intense thunderstorms over the foothills and hilly land.

Type	Taller 40 dBZ	More lightning	Count	FlRate	Maximum height			Pixels number			Ratio
					20 dBZ	30 dBZ	40 dBZ	20 dBZ	30 dBZ	40 dBZ	
Storm-A-type	Yes	No	359	14	15.3	14.4	11.8	116	63	24	0.90
Storm-B-type	Yes	Yes	261	82	16.1	15.2	12.3	542	327	107	0.85
Storm-C-type	No	Yes	474	55	14.1	12.6	9.6	1011	590	133	0.74